Bulletin of Engineering Geology and the Environment (2019) 78:4201–4215
https://doi.org/10.1007/s10064-018-1393-4

ORIGINAL PAPER

Landslide susceptibility mapping in the region of eastern Himalayan syntaxis, Tibetan Plateau, China: a comparison between analytical hierarchy process information value and logistic regression-information value methods

Guoliang Du[1] · Yongshuang Zhang[2] · Zhihua Yang[3] · Changbao Guo[3] · Xin Yao[3] · Dongyan Sun[1]

Received: 8 May 2018 / Accepted: 18 September 2018 / Published online: 4 October 2018

Abstract

The eastern Himalayan syntaxis in Tibet is one of the regions tectonically most active with the fastest uplift rate on the earth, where landslides are extremely frequent, causing severe damage to lives and transportation and inducing poverty. Thus, mapping landslide susceptibility of this area is of great importance. The purpose of this study is to compare landslide susceptibility maps for this region produced by the analytic hierarchy process information value (AHPIV) and logistic regression-information value (LRIV) methods using geographic information system (GIS) software. To do this, an inventory map with 799 landslides was prepared based on historical documents, interpretation of aerial photographs, and extensive field surveys. A total of eight conditioning factors were analyzed as input variables: lithology, slope gradient, slope aspect, elevation, curvature, distance to faults, distance to drainages and distance to roads. Then, the AHPIV and LRIV methods were applied to mapping landslide susceptibility. The performances of the methods were validated and compared using receiver operating characteristics (ROC) curves. The area under the curve (AUC) values obtained using the AHPIV and LRIV methods were 0.884, and 0.906, respectively. Results showed that the LRIV method performs better than the AHPIV method. Finally, sensitivity analyses were performed to examine the effects of removing any of the conditioning factors on the landslide susceptibility mapping. Results indicate that all of the conditioning factors have a positive effect on the landslide susceptibility mapping. Therefore, the LRIV method with eight conditioning factors was employed to determine potential landslide zones in the study area for landslide management and decision making.

Keywords Landslide susceptibility · GIS · Analytical hierarchy process information value · Logistic regression-information value · Eastern Himalayan syntaxis

✉ Yongshuang Zhang
zhys100@hotmail.com

Guoliang Du
756591925@qq.com

Zhihua Yang
yangzh99@163.com

Changbao Guo
guochangbao@cags.ac.cn

Xin Yao
yaoxinphd@163.com

Dongyan Sun
865320605@qq.com

[1] Hebei GEO University, No. 136 Huai An Road Yuhua District, Shijiazhuang 050031, China

[2] Tianjin Center, China Geological Survey, No. 4 Da Zhigu eight Road Hedong District, Tianjin 300170, China

[3] Key Laboratory of Neotectonic Movement and Geohazard, Institute of Geomechanics, Chinese Academy of Geological Sciences, 11A Minzu University Road Haidian District, Beijing 100081, China

Introduction

Landslides are defined as the mass movement of rock, debris or earth down a slope (Cruden 1991) that often cause great damages to human life, property and the natural environment in hilly and mountainous terrains. In active tectonic and erosional settings, landslides are generally considered the dominant hillslope process that permits rapid hillslope adjustment to high rates of rock uplift and erosion (Gallo and Lavé 2014). The eastern Himalayan syntaxis, located in the southeastern Tibetan Plateau, is one of the most tectonically active and fastest uplifting regions on Earth. Landslides are extremely developed in this region due to its special geological, tectonic and geomorphological conditions. Landslides along roads, especially National Highway 318, constantly result in loss of life and property damage (Shang et al. 2005), posing a serious challenge to project planning and construction. However, so far, no landslide susceptibility assessment has been made for this region.

As essential part of hazard assessment, landslide susceptibility mapping is one of most important ways to provide fundamental knowledge on landslide distribution and can help in hazard management. In the last three decades, a lot of techniques and methods have been applied to this effort, which can be roughly categorized into qualitative and quantitative ones (Ayalew and Yamagishi 2005).

The qualitative methods are based on field observations and prior knowledge of experts, in which experts identify judgment rules or assign weighted values for conditioning factor maps and then overlay them to prepare a landslide susceptibility map (Du et al. 2017a). They include the analytical hierarchy process (AHP; Ercanoglu et al. 2008; Ghosh et al. 2011; Kayastha et al. 2013) and weighted linear combination (WLC; Ayalew et al. 2004). Because the weights are assigned based on the field knowledge of experts, a landslide inventory map is not needed. The main problem of such qualitative methods is that they highly depend on the level of expert's experience, and any different criteria with the consent of the expert can easily be conceded to the assignment of weighted values (Feizizadeh et al. 2014).

The quantitative methods are based on numerical estimates and involve deterministic and statistical approaches (Bui et al. 2011). Deterministic methods are focused on analyzing the stability of a slope and calculating its safety factors (Aleotti and Chowdhury 1999; Godt et al. 2008; Park et al. 2013). Due to the need for exhaustive data from individual slopes, these methods are only applied to areas where landslide types are simple and the geomorphic and geologic properties are fairly homogeneous (Bui et al. 2011). Statistical methods are based on the analysis of the relationships between conditioning factors and existing landslides. These methods require the collection of a large amount of data to produce reliable results. Various statistical methods have been used for landslide susceptibility mapping including bivariate statistical analysis such as frequency ratio (FR; Lee and Pradhan 2006; Yilmaz and Keskin 2009; Mezughi et al. 2011; Regmi et al. 2014), information value (IV) method (Yin and Yan 1988; Lin and Tung 2004; Sarkar et al. 2008; Conforti et al. 2011), weight of evidence (WOE; Sharma and Kumar 2008; Suh et al. 2011; Guo et al. 2015), certainty factor (CF; Binaghi et al. 1998; Lan et al. 2004; Devkota et al. 2013), multivariate statistical analysis such as logistic regression (LR; Park 2010; Pourghasemi et al. 2013; Tsangaratos and Ilia 2016) and stepwise discriminant analyses (Carrara et al. 1991, 2003), and data mining methods such as artificial neural networks (ANNs; Arora et al. 2004; Yilmaz 2009; Pradhan and Lee 2010; Bui et al. 2016) and support vector machines (SVMs; Yao et al. 2008; Bui et al. 2016).

In addition, according to advantages of different methods, some integrated methods, such as LRFR (Umar et al. 2014; Youssef et al. 2015), AHPIV (Fan et al. 2012; Du et al. 2016), LRIV (Du et al. 2017a), AHPFR (Mondal and Maiti 2013), LRWOE (Zhou et al. 2016), have been developed to enhance precision and accuracy of landslide susceptibility mapping.

Although many methods and techniques have been proposed and implemented for landslide susceptibility mapping, there has been no consensus as to which method and technique are the best. In general, the performance of a method depends on characteristics of different regions (Yang et al. 2015). Thus, comparison of the different methods is important. Yilmaz (2010) compared the landslide susceptibility mapping results produced by LR, SVM and ANN methods and showed the ANN method produced more accurate susceptibility maps than LR and SVM for the case study of Koyulhisar, Turkey. Pourghasemi et al. (2013) compared landslide susceptibility mapping results using LR, AHP and statistical index (SI) for the north of metropolitan Tehran, Iran, and showed that the map obtained from the LR method is more accurate than the other methods. Chen et al. (2016) showed that the IV method enables generating a more accurate susceptibility map than LR for the Zigui-Badong area, China. In addition, the performance of the integrated method and the individual methods have been compared by some researchers. For example, Youssef et al. (2015) showed the LRFR method is better than the LR and FR methods in landslide susceptibility mapping. Zhou et al. (2016) considered that the LRWOE method can provide a more accurate result than the WOE and LR for earthquake-induced landslide susceptibility mapping based on a case study of the April 20, 2013 Lushan earthquake, China. Du et al. (2017a) showed the LRIV method can produce a more accurate susceptibility map than the LR and IV methods for the Bailongjiang watershed, Gansu Province, China. These integrated methods can yield a higher accuracy than individual methods for landslide susceptibility mapping.

Due to the complex topography of and difficult access to the region of the eastern Himalayan syntaxis, landsliding of this region is poorly studied, particularly in the Yarlung Zangbo Grand Canyon zone. To fill this gap, through aerial photograph interpretation and field investigations, we have prepared a landslide inventory map for this region, and then used the AHPIV and LRIV methods to generate a GIS-based landslide susceptibility map. Finally, the performances of the two methods are compared using the area under the receiver operating characteristic (ROC) curves.

Geologic settings

Associated with the collision between the Indian and Eurasian plates, the eastern Himalayan syntaxis is characterized by intensive tectonic deformation, with rapid uplift. This region is laced with many large-scale active faults, such as the Yarlung Zangbo fault, Jiali fault, Dongjiu-Milin fault, Polong-Pangxin fault, Apalong fault and Motuo fault, which control the topography and divide the region into different zones. The outcrop strata of the region range from the Proterozoic to Quaternary. In addition to the Jurassic and Quaternary strata, the others have all undergone different degrees of deterioration. The complex lithology in the region mainly consists of stone, limestone, marble, phyllite, slate, shale and basic, intermediate, intermediate-acidic and acidic magmatic rocks, as well as Quaternary alluvial, and diluvial or morainic materials.

In this region, the rapid uplift of the rock mass, surface erosion and river incision have created the current characteristics of the alpine gorge landscape. The research area is primarily of high mountains and valleys, with an average elevation of more than 3000 m and relative incision depth over 1000 m. Several mountain peaks above 6000 m stand here, such as the Namcha Barwa Peak as the highest one, with an elevation of 7782 m. Around the mountain peaks, the modern glaciers are well developed. The Yarlung Zangbo River basin is the largest watershed in the region, with several major tributaries including the Nyang River and Parlung Zangbo River. The Yarlung Zangbo River cuts through Namcha Barwa area and drops 2 km within the Yarlung Zangbo canyon (Du et al. 2017b). Along this great canyon, warm, moist air flows from the Indian Ocean to south Tibet, which brings abundant rainfall to the region. The annual rainfall is 700–1000 mm (Shang et al. 2005).

The tectonic rock uplifting, complex folding and faulting, coupled with river incision have produced special topographic, geomorphic and tectonic conditions for landslides in this region. Combined with the effect of gravity, earthquakes, rainfalls or glaciation can trigger frequent landslides of varied scales and types. These landslides are a serious challenge to the planning and construction of highways, railways and hydropower projects in this area.

Methodology

Analytic hierarchy process information value (AHPIV) method

Analytic hierarchy process (AHP)

As a multi-objective and multi-criteria decision-making approach, the AHP divides a complex decision-making problem into multiple objectives or criteria, expresses the subjective judgement in a quantitative manner and arrives at a scale of preference drawn from a set of alternatives, which makes the decision more reasonable. This method has been widely used in landslide susceptibility assessment (Mondal and Maiti, 2012). The AHP includes the following steps: (i) building a hierarchy model, (ii) establishing a judgment matrix through pairwise comparison (using a scale from 1 to 9), (iii) calculating weights by computation of the normalized principal eigenvector and (iv) testing consistency using the consistency ratio (CR) which must be less than 0.1. The CR is calculated by:

$$CR = \frac{CI}{RI} \tag{1}$$

$$CI = \frac{\lambda_{\max} - n}{n-1} \tag{2}$$

where CI is the consistency index, RI is the random consistency index, n is the number of parameters and λ_{max} is named the largest eigenvalue.

Information value (IV)

In the 1980s, Yin and Yan (1988) developed the IV method from information theory and used it in landslide spatial prediction for the first time. This method has been widely used since then, especially in landslide susceptibility assessment. It is an indirect statistical approach and can be used to evaluate the spatial relationship between the probability of landslide occurrence and conditioning factor classes (Du et al. 2017a). The information value of conditioning factor classes is calculated as follows (Yin and Yan 1988, 1996; Du et al. 2017a):

$$I_i = \log_2 \frac{S_i/A_i}{S/A} \tag{3}$$

where S_i is the area of landslides containing factor class i, A_i is the area of factor class i, S is total area of landslides and A is the total area of the entire study area (Yang et al. 2015; Du et al. 2017a).

AHPIV method

In the AHPIV method, the AHP is used to obtain the factor weights (w_i) and the information value method is used to obtain

the information value of the conditioning factor class (I_i). The integrated method can be expressed by the following formula:

$$I = \sum_{i=1}^{n} w_i I_i = \sum_{i=1}^{n} w_i \log_2 \frac{S_i/A_i}{S/A} \quad (4)$$

where I is the comprehensive index of the landslides occurrence, n is the number of the containing factor and w_i is the weight of the containing factor (Du et al. 2016; Wang et al. 2017).

Logistic regression information value (LRIV) method

Logistic regression (LR)

As one of the popular multivariate statistical analysis methods, LR can make a multivariate regression relationship between a binary dependent variable and numerous independent variables (Pradhan and Lee 2010). The advantage of LR is that the variables can be either continuous or discrete, or any combination of both types which need not be of a normal distribution (Lee and Pradhan 2006). The LR method has also been widely used in landslide susceptibility mapping. It can be expressed as:

$$P = \frac{1}{1 + e^{-z}} \quad (5)$$

where P is the probability of landslide occurrence, which varies from 0 to 1 on an S-shaped curve, and z is the linear combination of predictors and its value varies from $-\infty$ to $+\infty$ (Eq. 5).

$$z = \hat{\beta}_0 + \hat{\beta}_1 x_1 + \hat{\beta}_2 x_2 + \hat{\beta}_3 x_3 + \ldots\ldots + \hat{\beta}_n x_n \quad (6)$$

where $\hat{\beta}_0$ is the intercept of the model, n is the number of independent variables, $\hat{\beta}_i$ ($i = 1, 2, 3, \ldots, n$) represents coefficients of the model and x_i ($i = 1, 2, 3, \ldots, n$) is the independent variable.

LRIV method

The information value method was performed for all the classified conditioning factors. To speed up the convergence and facilitate the final analysis and interpretation in subsequent analysis, the information values should be normalized to a range of 0 to 1 (Du et al. 2017a). The normalized information values are then arranged to corresponding conditioning factor classes and used as independent variables in the LR model. These values can be calculated by a common method as follows:

$$x_i = \frac{I_i - I_{(i)\min}}{I_{(i)\max} - I_{(i)\min}} \quad (7)$$

$$z = \hat{\beta}_0 + \sum_{i=1}^{n} \hat{\beta}_i \cdot \frac{I_i - I_{(i)\min}}{I_{(i)\max} - I_{(i)\min}} \quad (8)$$

where x_i (independent variables in LR) is the normalized values of I_i, and $I_{(i)min}$ and $I_{(i)max}$ are the minimum and maximum information values of the ith conditioning factor, respectively (Du et al., 2017).

Landslide inventory

Landslide inventory mapping is the most basic step in landslide susceptibility assessment (Hong et al. 2018). A detailed and reliable landslide inventory with 799 landslides as polygons for the study area has been prepared based on interpretation of aerial photographs, extensive field surveys and historical landslide archives (scale: 1:100,000) compiled by the Ministry of Land and Resources of the People's Republic of China (Fig. 1). According to the material composition category (Liu et al. 2002), these landslides can be divided into two types: soil landslides and bedrock landslides. The soil landslides occurred primarily in the Quaternary loose material layers formed by alluvial deposits, residual slope deposits, collapse deposits, outwash deposits and artificial deposits. Most of them are distributed on the gentle slopes of the valleys. The bedrock landslides are associated with rock composition and structural weaknesses of slopes, which are widely distributed in the study area.

The size of the landslides ranges from several thousands to hundreds of millions cubic meters. Most of the large landslides ($>10^6$ m^3) are bedrock landslides in the study area. The giant landslide at Yigong in 2000 has an approximate length of 10 km and volume of 3.0×10^8 m^3 (Fig. 2a). Frequent landslides in this region, such as the 102 landslide (Fig. 2b), Layue landslide and Yigong landslide, have blocked rivers and caused serious damage to roads. Giant ancient landslides in the study area also prevail, such as the Jiaobunong landslide (Fig. 2c) and Wenlang landslide, which are mostly deep-seated. From the landslide inventory map, landslide distribution is of a certain regular pattern, mostly along the Yarlung Zangbo River, Parlung Zangbo River and Layue River (Fig. 1).

Landslide conditioning factors

In various references, there is still no clear agreement on the selection of conditioning factors in landslide susceptibility assessment (Hasekiogullari and Ercanoglu 2012; Guo et al. 2015). According to landslide characteristics of the study area, eight main landslide conditioning factors were chosen in this work, including lithology, slope gradient, slope aspect, elevation, curvature, distance to drainages, distance to faults and distance to roads. During map preparation, all of these factors were converted into raster format with a 30 × 30-m pixel size within the ArcGIS platform. They are detailed as follows, emphasized on their relations to landslide occurrence.

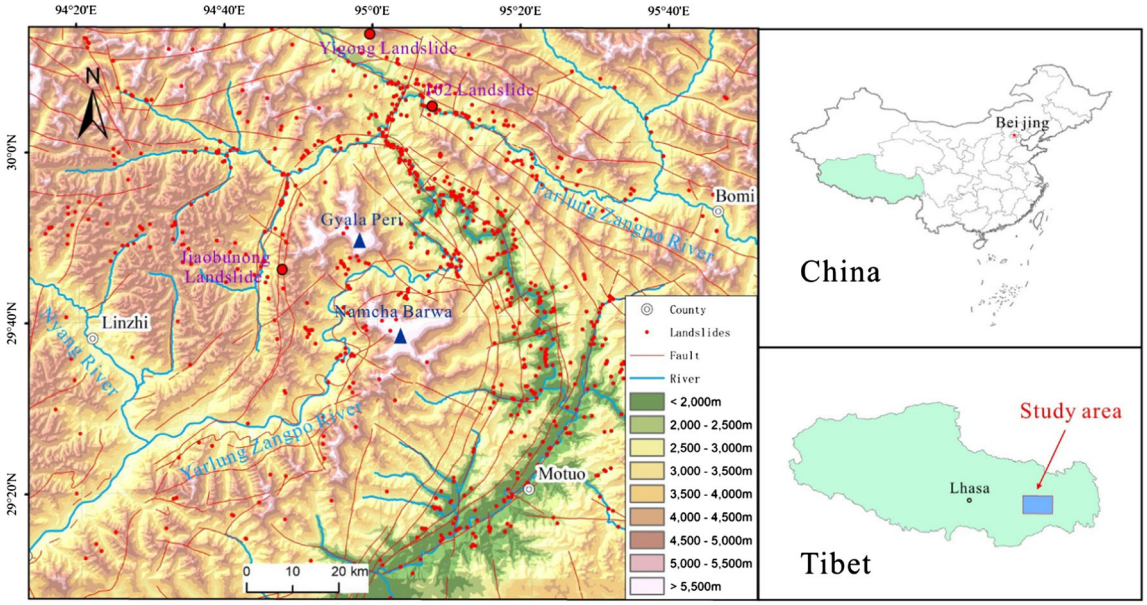

Fig. 1 Landslide inventory map of the study area

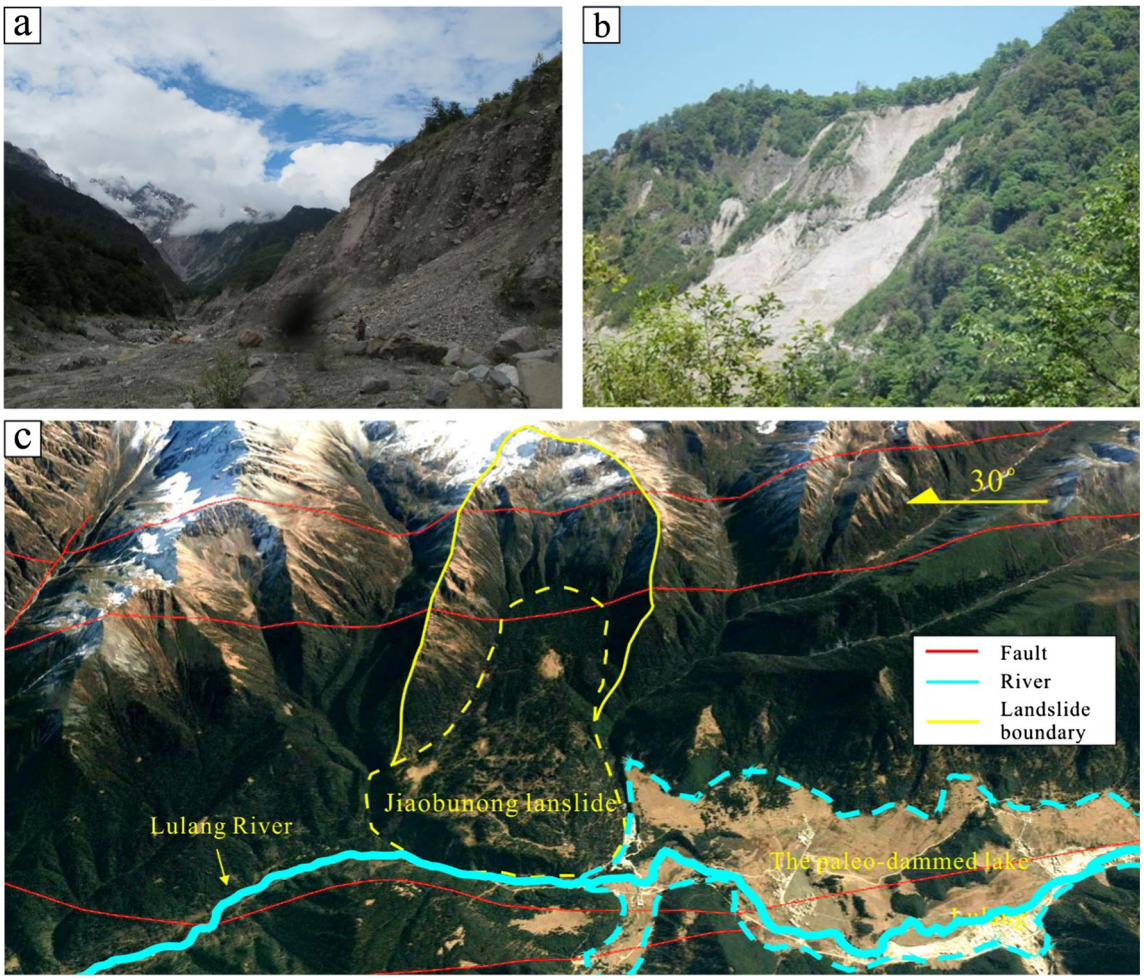

Fig. 2 Typical landslides in the study area. **a** Yigong landslide; **b** 102 landslide; **c** Jiaobunong ancient landslide

Lithology

Lithology is the material basis of landslide occurrence, which reflects the erodibility of the slope rock. Based on 1:200,000 geological maps produced by the Ministry of Land and Resources of China and physical-mechanical properties of rock, the lithology in the study area is divided into seven rock groups: (i) hard solid granite and diorite, (ii) hard layer of sandstone and limestone, (iii) mid-hard solid migmatites, (iv) mid-hard layer of basic-ultrabasic rocks, (v) soft-hard layer of schist and gneiss, (vi) loose sediments and (vii) snow-covered region (Fig. 3a). In the study area, the groups of mid-hard layer of basic-ultrabasic rocks and soft-hard layer of schist and gneiss are relatively more prone to landsliding. The highest density of landslides is present in the group of mid-hard layer of basic-ultrabasic rocks which are mainly distributed along the Yarlung Zangbo suture zone (Fig. 4a). Due to the compression of the Namche Barwa wedge and Gangdise-Nyainqentanglha block, rock mass in this zone is highly broken, serving as a favorable condition for landslide occurrence.

Slope gradient

Slope gradient, which affects the gravity-generated stress distribution, surface runoff and the loose material accumulation of the slope, plays an important role in landsliding. In this work, this parameter was obtained from the 30 × 30-m digital elevation model (DEM) and divided into six classes: <10°, 10–20°, 20–30°, 30–40°, 40–50° and >50° (Fig. 3b). The occurrence of landslides within each class in the study area is described in Fig. 4b and Table 1. It is noted that most of these landslides occurred on slopes of 20–50°. The lowest frequencies of landslides were on the very gentle slopes (0–10°).

Slope aspect

Slope aspect plays an important role in landslide susceptibility mapping, which is related to weathering, land cover and microclimate. Many scholars use slope aspect as a conditioning factor in landslide susceptibility mapping (Meinhardt et al. 2015; Youssef et al. 2015; Chen et al. 2017). The values of this parameter were also derived from the 30 × 30-m DEM and categorized into nine classes: flat, N, NE, E, SE, S, SW, W and NW (Fig. 3c). Figure 4c shows that landslides are likely to occur on the slopes facing west, southwest and south.

Elevation

Related to soil types, vegetation coverage, rainfall and so on, elevation can influence the landslide distribution. This factor in the study area is divided into eight classes: <2000 m, 2000–2500 m, 2500–3000 m, 3000–3500 m, 3500–4000 m, 4000–4500 m, 4500–5000 m and > 5000 m (Fig. 3d). The spatial relationship between landslides and elevation classes (Fig. 4d) suggests that the slope failures in the study area mainly occurred at places with elevation of <2500 m, which are mostly catchment areas with strong surface runoff, seeming more prone to landsliding.

Fig. 3 Maps of landslide conditioning factors. **a** Lithology: (i) hard solid granite and diorite, (ii) hard layer of sandstone and limestone, (iii) mid-hard solid migmatites, (iv) mid-hard layer of basic-ultrabasic rocks, (v) soft-hard layer of schist and gneiss, (vi) loose sediments and (vii) snow-covered region; **b** slope gradient (°); **c** slope aspect; **d** elevation (m); **e** curvature; **f** distance to faults (m); **g** distance to drainages (m); **h** distance to roads (m). Maps of landslide conditioning factors (continued)

Curvature

Curvature is another DEM-based derivative, which can affect slope stress field and groundwater distribution. Many researchers use slope curvature as a conditioning factor in preparing landslide susceptibility maps (Umar et al. 2014; Guo et al. 2015; Chen et al. 2017). The slope curvature map was prepared with three classes: concave, flat and convex (Fig. 3e). Figure 4e and Table 1 show that the highest landslide density and area occurred at the localities of convex curvature, followed by area of flat and concave curvatures.

Distance to faults

The faults data are based on 1:200,000 geological maps. Apparently, with well-developed cracks, fragmented rock and strong weathering, the slope on both sides of the faults is highly susceptible to landslides. In this work, the distance to faults was calculated in a 500-m interval and is divided into nine classes: <500 m, 500–1500 m, 1000–1500 m, 1500–2000 m, 2000–2500 m, 2500–3000 m, 3000–3500 m, 3500–4000 m and >4000 m (Fig. 3f). The landslide distribution is obviously controlled by the faults, as evidenced by the landslide density decreasing with increasing distance to the faults within 3000 m (Fig. 4f).

Distance to drainages

River undercutting, infiltration and erosion are unfavorable for slope stability along the river banks. The growth level of the surface drainages indicates the cutting level of the surface. The more developed the water system, the more severe the surface cutting. Meng et al. (2004) argued that the rapid uplift of the Tibetan Plateau during the Late Quaternary period led to strong river incision, and thus controlled geological hazards and their distribution. For the study area, the distance to drainages is divided into nine classes: <100 m, 100–200 m, 200–300 m, 300–400 m, 400–500 m, 500–600 m, 600–700 m, 700–800 m

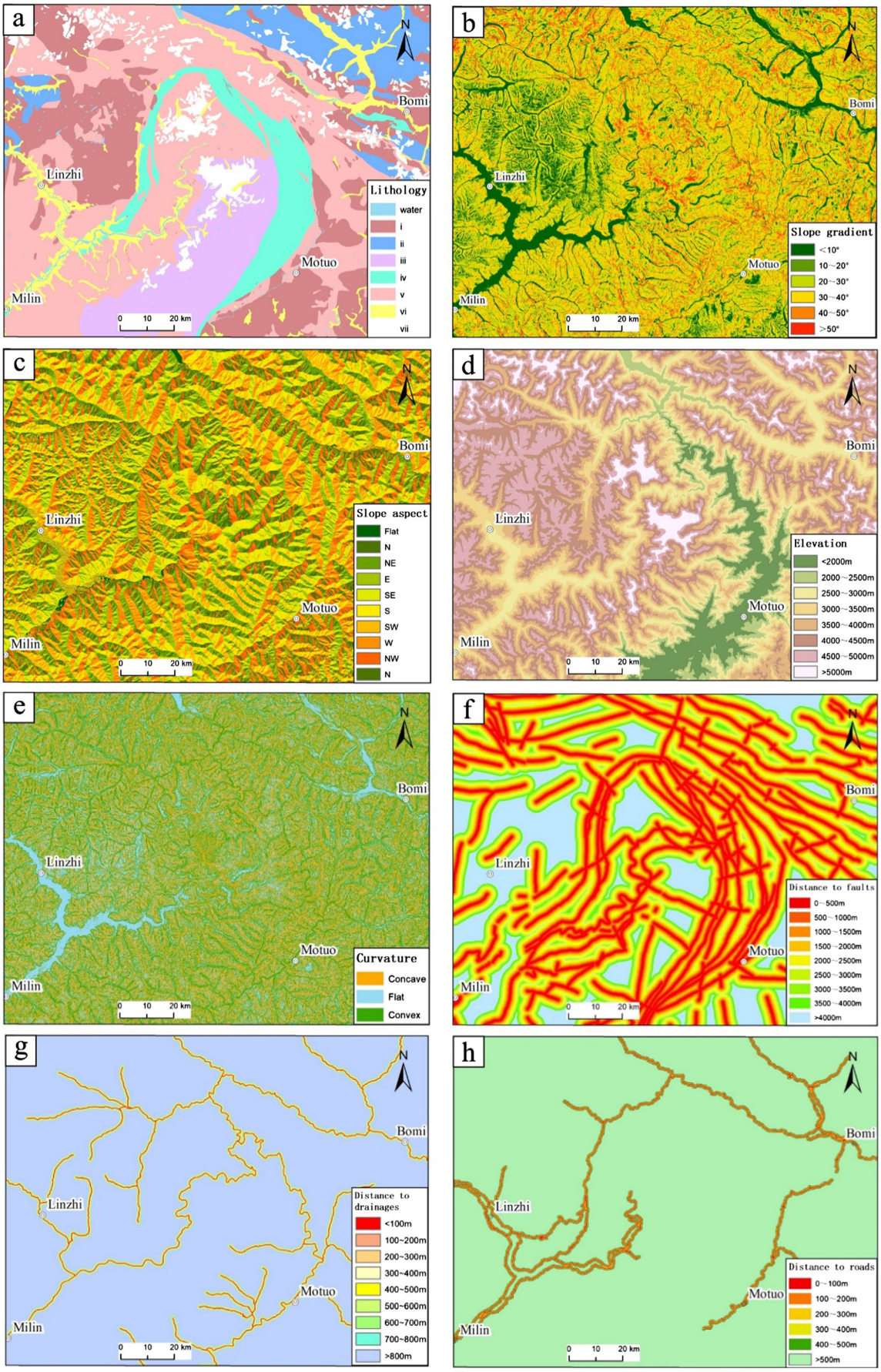
a
N
Bomi
Linzhi
Motuo
Milin
Lithology
water
i
ii
iii
iv
v
vi
vii
0 10 20 km
b
N
Bomi
Linzhi
Motuo
Milin
Slope gradient
<10°
10~20°
20~30°
30~40°
40~50°
>50°
0 10 20 km
c
N
Bomi
Linzhi
Motuo
Milin
Slope aspect
Flat
N
NE
E
SE
S
SW
W
NW
N
0 10 20 km
d
N
Bomi
Linzhi
Motuo
Milin
Elevation
<2000m
2000~2500m
2500~3000m
3000~3500m
3500~4000m
4000~4500m
4500~5000m
>5000m
0 10 20 km
e
N
Bomi
Linzhi
Motuo
Milin
Curvature
Concave
Flat
Convex
0 10 20 km
f
N
Bomi
Linzhi
Motuo
Milin
Distance to faults
0~500m
500~1000m
1000~1500m
1500~2000m
2000~2500m
2500~3000m
3000~3500m
3500~4000m
>4000m
0 10 20 km
g
N
Bomi
Linzhi
Motuo
Milin
Distance to drainages
<100m
100~200m
200~300m
300~400m
400~500m
500~600m
600~700m
700~800m
>800m
0 10 20 km
h
N
Bomi
Linzhi
Motuo
Milin
Distance to roads
0~100m
100~200m
200~300m
300~400m
400~500m
>500m
0 10 20 km

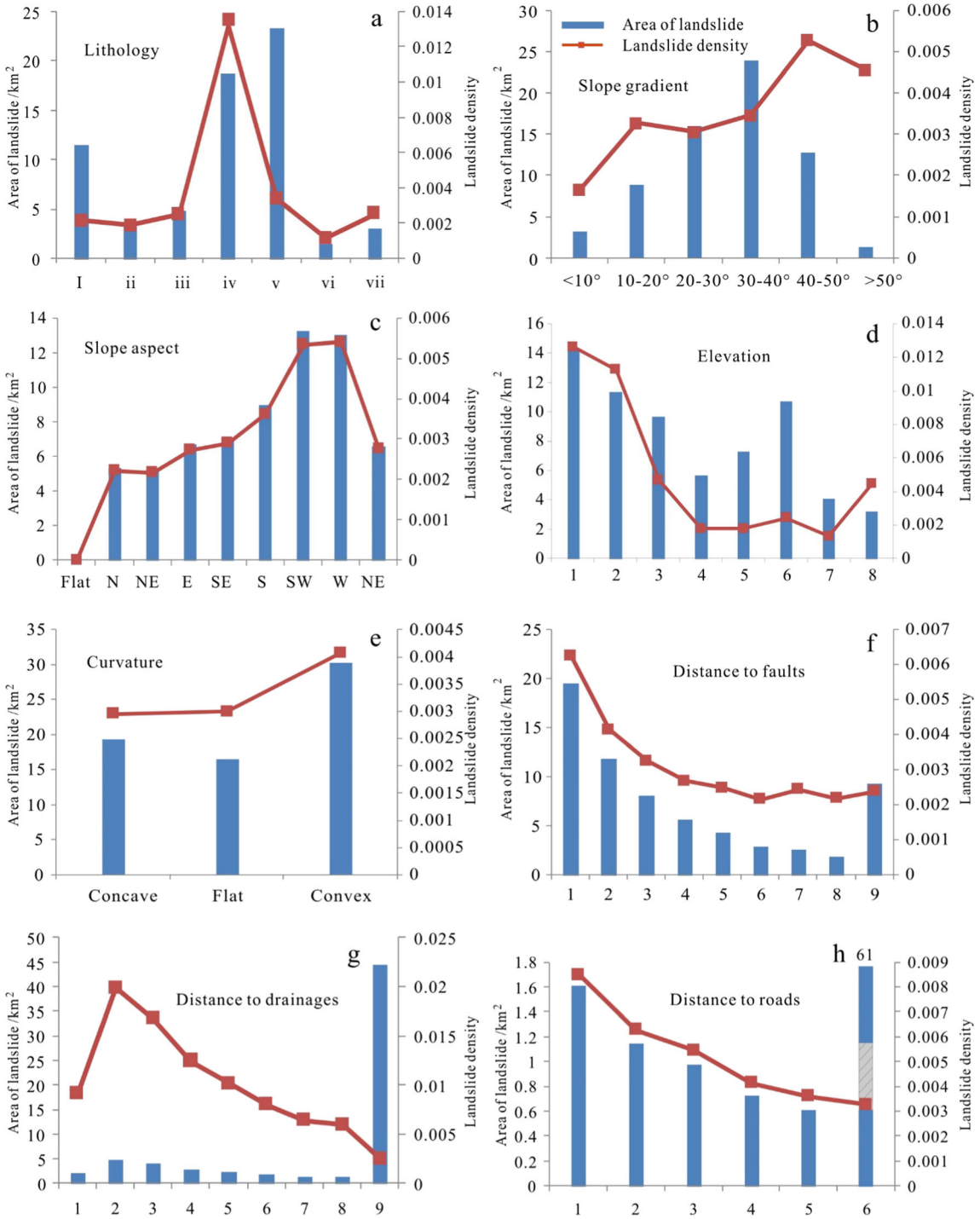

Fig. 4 Relationships between landslide occurrence and conditioning factor classes. **a** Lithology: (i) hard solid granite and diorite, (ii) hard layer of sandstone and limestone, (iii) mid-hard solid migmatites, (iv) mid-hard layer of basic-ultrabasic rocks, (v) soft-hard layer of schist and gneiss, (vi) loose sediments and (vii) snow-covered region; **b** slope gradient (°); **c** slope aspect; **d** elevation: (1) <2000 m, (2) 2000~2500 m, (3) 2500~3000 m, (4) 3000~3500 m, (5) 3500~4000 m, (6) 4000~4500 m, (7) 4500~5000 m and (8) >5000 m; **e** curvature; **f** distance to faults: (1) <500 m, (2) 500~1500 m, (3) 1000~1500 m, (4) 1500~2000 m, (5) 2000~2500 m, (6) 2500~3000 m, (7) 3000~3500 m, (8) 3500~4000 m and (9) >4000 m; **g** distance to drainages: (1) <100 m, (2) 100~200 m, (3) 200~300 m, (4) 300~400 m, (5) 400~500 m, (6) 500~600 m, (7) 600~700 m, (8) 700~800 m and (9) >800 m; **h** distance to roads: (1) <100 m, (2) 100~200 m, (3) 200~300 m, (4) 300~400 m, (5) 400~500 m and (6) >500 m

and > 800 m (Fig. 4f). Figure 4g shows that the landslide density is the largest in the distance class of 100–200 m, and declines with the growing distance to drainages when exceeding 200 m.

Table 1 Spatial relationships between each landslide conditioning factor and landslides

Conditioning factor	Class	Area of pixels in domain(m^2)	Percentage of domain (%)	Area of landslide(m^2)	Percentage of and landslide (%)	Information value
Lithology	i	5,162,060,700	26.44	11,508,300	17.34	−0.6085
	ii	1,684,039,500	8.62	3,282,300	4.95	−0.5562
	iii	1,947,306,600	9.97	4,923,900	7.42	−0.2958
	iv	1,419,343,200	7.27	18,778,500	28.29	1.3590
	v	6,865,775,100	35.16	23,358,600	35.19	0.0009
	vi	1,258,597,800	6.45	1,461,600	2.20	−1.0740
	vii	1,189,447,200	6.09	3,059,100	4.61	−0.2789
Slope gradient	<10°	1,969,734,600	10.09	3,275,100	4.93	−0.7151
	10–20°	2,705,940,000	13.86	8,883,000	13.38	−0.0348
	20–30°	5,229,216,000	26.78	16,020,900	24.14	−0.1039
	30–40°	6,884,020,800	35.25	23,937,400	36.07	0.0227
	40–50°	2,425,848,300	12.42	12,826,800	19.33	0.4419
	>50°	311,810,400	1.60	1,429,100	2.15	0.2989
Slope aspect	Flat	53,390,700	0.27	0	0.00	–
	N	2,405,283,300	12.32	5,355,000	8.07	−0.4231
	NE	2,434,949,100	12.47	5,304,600	7.99	−0.4449
	E	2,456,188,200	12.58	6,715,800	10.12	−0.2177
	SE	2,419,929,900	12.39	7,043,400	10.61	−0.1552
	S	2,476,841,400	12.68	8,999,100	13.56	0.0666
	SW	2,482,023,600	12.71	13,284,000	20.01	0.4540
	W	2,414,651,400	12.37	13,058,100	19.67	0.4644
	NW	2,383,312,500	12.21	6,612,300	9.96	−0.2031
Elevation	<2000 m	1,123,910,100	5.76	14,206,600	21.40	1.3134
	2000–2500 m	1,006,851,600	5.16	11,379,500	17.14	1.2015
	2500–3000 m	2,058,228,900	10.54	9,702,000	14.62	0.3270
	3000–3500 m	3,135,868,200	16.06	5,674,500	8.55	−0.6304
	3500–4000 m	4,021,956,900	20.60	7,283,700	10.97	−0.6296
	4000–4500 m	4,387,375,800	22.47	10,746,900	16.19	−0.3276
	4500–5000 m	3,065,797,800	15.70	4,121,100	6.21	−0.9277
	>5000 m	726,580,800	3.72	3,258,000	4.91	0.2770
Curvature	Concave	6,540,729,300	33.50	19,359,900	29.17	−0.1383
	Flat	5,550,660,000	28.43	16,641,900	25.07	−0.1255
	Convex	7,435,180,800	38.08	30,370,500	45.76	0.1837
Distance to faults	<500 m	3,133,632,600	16.05	19,578,600	29.50	0.6087
	500–1000 m	2,862,952,200	14.66	11,869,200	17.88	0.1986
	1000–1500 m	2,489,009,400	12.75	8,132,400	12.25	−0.0395
	1500–2000 m	2,094,750,000	10.73	5,634,900	8.49	−0.2340
	2000–2500 m	1,719,324,900	8.81	4,295,700	6.47	−0.3078
	2500–3000 m	7,226,901,000	6.95	2,938,500	4.43	−0.4505
	3000–3500 m	1,356,423,300	5.48	2,619,000	3.95	−0.3287
	3500–4000 m	1,070,318,700	4.52	1,937,700	2.92	−0.4367
	>4000 m	882,201,600	20.06	9,366,300	14.11	−0.3520
Distance to drainages	<100 m	249,705,000	1.28	2,296,800	3.46	0.9955
	100–200 m	247,788,000	1.27	4,928,400	7.43	1.7667
	200–300 m	245,519,100	1.26	4,122,000	6.21	1.5972
	300–400 m	243,260,100	1.25	3,037,500	4.58	1.3012
	400–500 m	241,539,300	1.24	2,456,100	3.70	1.0958
	500–600 m	238,821,300	1.22	1,912,500	2.88	0.8569
	600–700 m	236,813,400	1.21	1,525,500	2.30	0.6393
	700–800 m	234,561,600	1.20	1,405,800	2.12	0.5671
	>800 m	17,588,562,300	90.08	44,687,700	67.33	−0.2911
Distance to roads	<100 m	189,393,300	0.97	1,612,800	2.43	0.9184
	100–200 m	182,605,500	0.94	1,148,400	1.73	0.6153
	200–300 m	178,782,300	0.92	979,200	1.48	0.4771
	300–400 m	175,050,900	0.90	726,300	1.09	0.1994
	400–500 m	170,227,800	0.87	613,900	0.92	0.0592
	>500 m	18,630,510,300	95.41	61,291,700	92.35	−0.0327
Total area		19,526,570,100		66,372,300		

Note: Percentage of domain = area of pixels in domain/total area of pixels; percentage of and landslide = area of landslide/total area of landslide

Distance to roads

Due to the micromorphological changes and unloading by road excavation, the slope instabilities often occur along roads in mountainous areas. In addition, the human engineering activities are also generally along roads. These constitute an influence factor for slope failures which depend on the distance to the road. In this work, this parameter was calculated in 500-m intervals and is divided into six classes: <100 m, 100–200 m, 200–300 m, 300–400 m, 400–500 m and > 500 m (Fig. 3h). Analysis shows that in the study area, the landslide density is highest at distances of 0 to 100 m to roads, while lowest for the distances >500 m. The landslide density decreases with the increasing distance to the roads (Fig. 4h).

Results

Landslide susceptibility map using AHPIV

In this method, the judgment matrix (Table 2) was established by the pairwise comparison. The weight values of eight conditioning factors were determined and the consistency test was carried out (Table 2). The CR is 0.025, which is less than 0.1. The results indicated that the judgement matrix satisfies the requirement of the consistency test and the weight values are reasonable.

The information values of eight conditioning factors (I_{li} = lithology, I_{sl} = slope gradient; I_{as} = slope aspect; I_{ss} = curvature; I_{el} = elevation; I_{fa} = distance to faults; I_{ri} = distance to drainages; I_{ro} = distance to roads) were calculated using Eq. 3. The information values are listed in Table 1. To obtain the landslide susceptibility index, the weight values for each conditioning factor (Table 2) were placed in Eq. 9. Finally, the landslide susceptibility results were divided into five categories using the natural breakpoint method, which are very low, low, moderate, high and very high landslide susceptibility (Fig. 5a).

$$I = 0.169I_{\mathrm{li}} + 0.259I_{\mathrm{sl}} + 0.065I_{\mathrm{as}} + 0.051I_{\mathrm{ss}} + 0.076I_{\mathrm{el}} + 0.132I_{fa} + 0.154I_{ri} + 0.094I_{\mathrm{road}} \quad (9)$$

Landslide susceptibility map using LRIV

In order to avoid the bias caused by unequal proportions of landslide and non-landslide pixels when implementing this method, an equal grid cell of non-landslides was randomly selected from the landslide-free area (Bui et al. 2011). The normalized information value layers of conditioning factors were calculated using Eqs. 3 and 7. By analyzing the relationship between the dependent variables (0 is the value of non-landslide and 1 is the landslide) and independent variables (the normalized information values) in SPSS statistics software, the LR coefficients of conditioning factors were obtained. Then, substituting LR coefficients into Eq. 8, the z values were obtained as follows:

$$z = -5.788 + 2.015I_{\mathrm{li}} + 4.747I_{\mathrm{sl}} + 1.787I_{\mathrm{as}} + 2.501I_{\mathrm{ss}} + 0.125I_{\mathrm{el}} + 0.981I_{fa} + 1.492I_{ri} + 0.241I_{\mathrm{road}} \quad (10)$$

The P values, which ranged from 0.0194 to 0.9869, were obtained by substituting the z values into Eq. 5. To prepare the landslide susceptibility map, the P value map was divided into five classes using the natural breakpoint method, which are very low, low, moderate, high and very high landslide susceptibility (Fig. 5b).

In order to avoid the multicollinearity among the independent variables, a collinearity analysis is necessary. Tolerance

Table 2 Results of the AHP evaluation

Conditioning factor	Lithology	Slope gradient	Slope aspect	Curvature	Elevation	Distance to faults	Distance to drainages	Distance to roads
Lithology	1	1/2	3	3	2	2	1	2
Slope gradient	2	1	4	4	3	2	2	3
Slope aspect	1/3	1/4	1	1	2	1/3	1/3	1/2
Curvature	1/3	1/4	1	1	1/2	1/3	1/3	1/2
Elevation	1/2	1/3	1/2	2	1	1/2	1/2	1
Distance to faults	1/2	1/2	3	3	2	1	1	1
Distance to drainages	1	1/2	3	3	2	1	1	2
Distance to roads	1/2	1/3	2	2	1	1	1/2	1
Weight values	0.169	0.259	0.065	0.051	0.076	0.132	0.154	0.094
Consistency test	CI = 0.035, CR = 0.025 < 0.1							

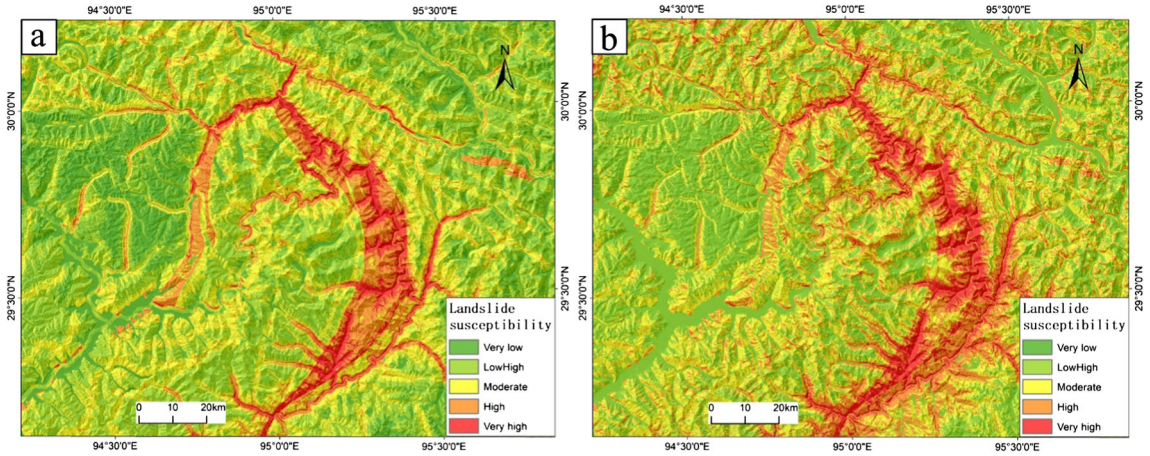

Fig. 5 Landslide susceptibility maps produced by (**a**) AHPIV and (**b**) LRIV methods

(TOL) and variance inflation factor (VIF) are two primary indexes to assess the multicollinearity (Bui et al. 2011). When the TOL is less than 0.1 or the VIF greater than 10, it is regarded as a multicollinearity problem existing. The TOL and VIF values (Table 3) show that there is no multicollinearity among the chosen independent variables. Table 3 lists the *P* value of each logistic coefficient in the model. It shows that all the conditioning factors have a *P* value less than 0.05, which demonstrates that the statistical relationship between variables at a 95% confidence level (Bui et al. 2011). All these indicate that the presented model performs quite well.

Validation

Validation is a fundamental step to assess the effectiveness of the landslide susceptibility map. In this study, the ROC curve was used to verify the performance of the landslide susceptibility map. This curve is a two-dimensional graph that consists of the true positive rate (sensitivity) on the vertical axis and false positive rate (1 = specific) on the horizontal axis. The area under the ROC curve (AUC), which varies from 0.5 to 1.0, is used to evaluate the model. An AUC value close to the 1.0 implies perfect performance of the model (Bui et al. 2011; Umar et al. 2014).

The ROC curve results showed that the AUC is 0.906 using the LRIV method and 0.884 using the AHPIV method (Fig. 6). It is evident that the LRIV method can produce a better landslide susceptibility map than the AHPIV method in the study area. Figure 7 show the landslide density and area for the five landslide susceptibility classes of the two landslide susceptibility maps, on which the landslide density decreases with lowering the landslide susceptibility.

Table 3 Relevant parameters of conditioning factors used in LRIV method

Conditioning factor	TOL	VIF	Logistic coefficient	*P* value
Lithology	0.7973	1.2543	2.0150	0.0000
Slope gradient	0.8387	1.1923	4.7473	0.0000
Slope aspect	0.9788	1.0216	1.7868	0.0000
Elevation	0.6746	1.4823	2.5045	0.0000
Curvature	0.9712	1.0297	0.1251	0.0000
Distance to faults	0.8670	1.1534	0.9813	0.0000
Distance to drainages	0.6084	1.6437	1.4917	0.0000
Distance to roads	0.8096	1.2352	0.2407	0.0001
Constant			−5.7876	0.0000

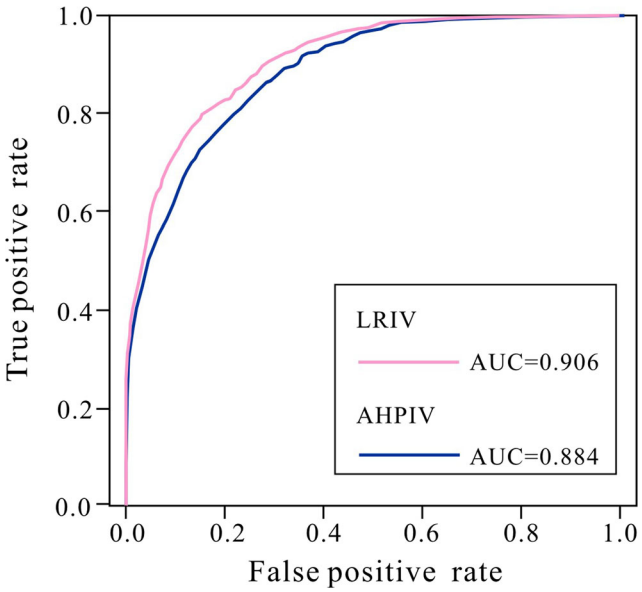

Fig. 6 Receiver operating characteristic (ROC) curve

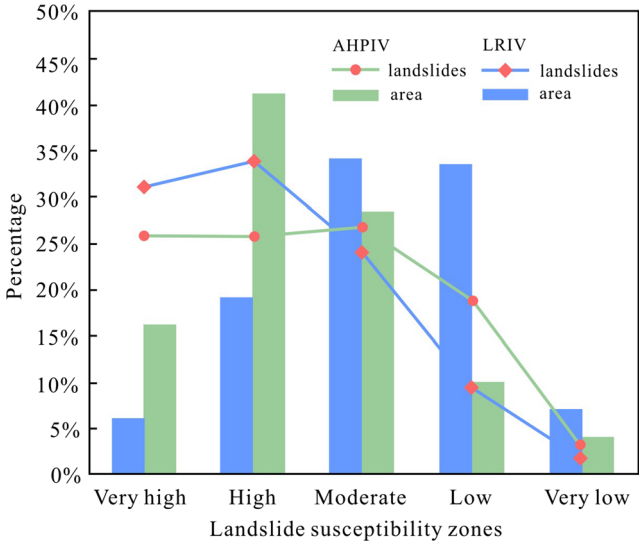

Fig. 7 Statistics of the landslide susceptibility map produced by the AHPIV and LRIV methods

Sensitivity analysis

Sensitivity analysis permits seeing how the input variables change the output results (Lee and Talib 2005; Fenta et al. 2015; Tahmassebipoor et al. 2016; Du et al. 2017a). In this study, a map-removal sensitivity analysis (Tahmassebipoor et al. 2016) was conducted to examine the effects of removing any of the conditioning factors on the landslide susceptibility results. The relative decrease of AUC values (RD), which is used to examine the solution changes, is calculated as follows:

$$RD_i = \frac{AUC_{\text{all}} - AUC_i}{AUC_{\text{all}}} \times 100\% \quad (11)$$

where RD_i is the relative decrease of AUC values, AUC_{all} is the AUC value obtained from the landslide susceptibility mapping using all conditioning factors and AUC_i is the AUC value when the *i*th conditioning factor is excluded. A high *RD* value means a high sensitivity to a landslide susceptibility resulted.

Removing each of conditioning factors in turn, the landslide susceptibility assessment was performed using the LRIV method (Table 4) and the corresponding RD value was calculated. The sensitivity analysis (Table 5) shows that the lithology (RD = 3.02%), slope gradient (RD = 12.05%), aspect (RD = 2.99%), elevation (RD = 2.56%), curvature (RD = 2.26%), distance to drainages (RD = 4.15%), distance to faults (RD = 2.65%) and distance to roads (RD = 2.24%) all have a decline in AUC values. The landslide susceptibility map is more sensitive to the slope gradient and less sensitive to the distance to roads in the study area.

From the results of ROC and sensitivity analysis, it can be concluded that the landslide susceptibility assessment performance is affected not only by the method used, but also by the type and the number of conditioning factors selected.

Hence, we produced the landslide susceptibility map of the eastern Himalayan syntaxis region using the LRIV method with all eight conditioning factors. From the statistical results of the landslide susceptibility map (Table 6), the very high and high landslide susceptibility areas, accounting for 5.98 and 19.10% of the entire area, respectively, are mainly distributed along the narrow valleys of the Yarlung Zangbo, Yigong Zangbo, Parlung Zangbo and Layue Rivers. The moderate landslide susceptibility areas, accounting for 34.33% of the whole study area, are mainly distributed along tributary gullies of the major rivers. Table 6 shows that 23.96% of the landslides occur in these areas, whereas only 10.88% of the landslides are present in the areas with low and very low landslide susceptibility, which accounts for 40.59% of the study area. The low and very low landslide susceptibility zones are mainly in the areas with gentle slopes and less faults.

Table 4 Regression coefficients of the logistic regression-information value method when the relevant conditioning factor is excluded

Excepted factor	β_1	β_2	β_3	β_4	β_5	β_6	β_7	β_8	β_0
Lithology	–	5.048	1.743	2.510	0.090	1.252	1.418	−0.095	−5.169
Slope gradient	2.965	–	2.093	2.276	0.309	0.516	1.475	−0.243	−3.878
Slope aspect	1.971	4.836	–	2.482	0.117	0.972	1.452	0.166	−4.507
Elevation	2.059	4.724	1.778	–	0.141	1.196	2.477	0.318	−5.121
Curvature	2.007	4.761	1.784	2.506	–	0.983	1.508	0.237	−5.740
Distance to faults	2.257	4.623	1.776	2.608	0.134	–	1.592	.279	−5.508
Distance to drainages	1.962	4.728	1.759	2.855	.167	1.041	–	1.267	−5.778
Distance to roads	2.006	4.742	1.784	2.507	0.125	0.983	1.554	–	−5.779

Table 5 Statistics of the sensitivity analysis

Excepted factor	Success rate value	Decrease of success rate value (%)
Lithology	0.8786	3.02
Slope gradient	0.7969	12.05
Slope aspect	0.8789	2.99
Elevation	0.8828	2.56
Curvature	0.8855	2.26
Distance to faults	0.8820	2.65
Distance to drainages	0.8684	4.15
Distance to roads	0.8857	2.24

Discussion and conclusions

The IV method is a simple and effective tool in landslide susceptibility mapping. Among all bivariate statistical methods, this approach can determine the impact of each conditioning factor class on landslide occurrence, but it does not consider the relationship between these factors and landslide occurrence (Du et al. 2017a). The LR method is capable of performing multivariate statistical analysis between a dependent variable and several independent ones and provides an easy way to analyze the impact of conditioning factors on landslide occurrence, but it does not analyze the influence of classes of each conditioning factor on landslides (Umar et al. 2014). As a main tool in the subjective assessment of qualitative methods, the AHP method can assign the weights of conditioning factors based on the field knowledge of experts. But this method may be strongly influenced by the subjectivity of the involved experts (Bui et al.2011). The AHP and LR methods can be combined with bivariate statistical analysis (BSA) methods such as the IV method (Umar et al. 2014; Yang et al. 2015; Du et al. 2017a). This study produced landslide susceptibility maps in the region of the eastern Himalayan syntaxis using two integrated methods: the AHPIV method and the LRIV method. The methods can generate a complete model to assess the impact of conditioning factors as well as the effect of each conditioning factor on landslide occurrence. However, the AHPIV method assesses the impact of conditioning factors on landslide occurrence based on field observations and prior knowledge of experts, and the LRIV method does the same by virtue of numerical estimates. The performance of susceptibility maps produced by these two methods for the study area was verified by the ROC curves. The AUC value for the LRIV method is 0.906, which is better than the 0.884 of the AHPIV method. The results indicate that the LRIV method is the best optimized model in this study and it can be considered as a promising method for landslide susceptibility mapping in similar cases for better accuracy.

It is worth noting that the conditioning factors play a key role in landslide susceptibility mapping, but there is no universal standard on how to select conditioning factors and how many factors should be selected. Guo et al. (2015) found that the FR model with the 6 variables performed the same as that with the all 11 variables, and better than 8 variables. Meinhardt et al. (2015) compared landslide susceptibility map results using 9 and 13 variables and found that 9 variables led to a higher AUC value than those from all 13 variables. In this study, we considered eight factors for analysis. The sensitivity analyses were performed to find a better input parameter set, and the results showed that all of the conditioning factors had a positive effect on the landslide susceptibility mapping. However, due to the difficulty of obtaining data, other factors such as rainfall, ground water level and weathering that affect the landslide occurrence are not considered. Whether choosing more factors is conducive to landslide susceptibility results of the study area needs further research.

From this study, we suggest using the LRIV method with all eight conditioning factors to map the landslide susceptibility. This paper gives in-depth thought about landslide susceptibility mapping and the results can help managers, planners and decision makers in land use, landslide management and landslide hazard prevention and mitigation in engineering construction.

Table 6 Statistics of the landslide susceptibility map

Landslide susceptibility zone	Pixel number	Percentage of area (%)	Area of landslide (m^2)	Percentage of landslide (%)
Very high	1,297,349	5.98	20,657,700	31.12
High	4,143,673	19.10	22,590,000	34.04
Moderate	7,448,786	34.33	15,901,200	23.96
Low	7,257,956	33.45	6,190,200	9.33
Very low	1,548,425	7.14	1,033,200	1.55

Acknowledgements This study is supported by the National Natural Science Foundation of China (41731287, 41807231) and China Geological Survey Project (12120113038000).

References

Aleotti P, Chowdhury R (1999) Landslide hazard assessment: summary review and new perspectives. Bull Eng Geol Environ 58(1):21–44

Arora MK, Das Gupta AS, Gupta RP (2004) An artificial neural network approach for landslide hazard zonation in the Bhagirathi (Ganga) valley, Himalayas. Int J Remote Sens 25(3):559–572

Ayalew L, Yamagishi H (2005) The application of GIS-based logistic regression for landslide susceptibility mapping in the Kakuda-Yahiko Mountains, Central Japan. Geomorphology 65(1–2):15–31

Ayalew L, Yamagishi H, Ugawa N (2004) Landslide susceptibility mapping using GIS-based weighted linear combination, the case in Tsugawa area of Agano River, Niigata prefecture, Japan. Landslides 1(1):73–81

Binaghi E, Luzi L, Madella P et al (1998) Slope instability zonation: a comparison between certainty factor and fuzzy Dempster-Shafer approaches. Nat Hazards 17(1):77–97

Bui DT, Lofman O, Revhaug I et al (2011) Landslide susceptibility analysis in the Hoa Binh province of Vietnam using statistical index and logistic regression. Nat Hazards 59(3):1413–1444

Bui DT, Tuan TA, Klempe H et al (2016) Spatial prediction models for shallow landslide hazards: a comparative assessment of the efficacy of support vector machines, artificial neural networks, kernel logistic regression, and logistic model tree. Landslides 13(2):361–378

Carrara A, Cardinali M, Detti R, Guzzetti F, Pasqui V, Reichenbach P (1991) GIS techniques and statistical models in evaluating landslide hazard. Earth Surf Process Landf 16(5):427–445

Carrara A, Crosta G, Frattini P (2003) Geomorphological and historical data in assessing landslide hazard. Earth Surface Proc Landform: J Bri Geomorphol Res Group 28(10):1125–1142

Chen T, Niu R, Jia X (2016) A comparison of information value and logistic regression models in landslide susceptibility mapping by using GIS. Environ Earth Sci 75(10):1–16

Chen W, Xie X, Wang J, Pradhan B et al (2017) A comparative study of logistic model tree, random forest, and classification and regression tree models for spatial prediction of landslide susceptibility. Catena 151:147–160

Conforti M, Aucelli PPC, Robustelli G et al (2011) Geomorphology and GIS analysis for mapping gully erosion susceptibility in the Turbolo stream catchment (northern Calabria, Italy). Nat Hazards 56(3):881–898

Cruden DM (1991) A simple definition of a landslide. Bull Int Assoc Eng Geol 43(1):27–29

Devkota KC, Regmi AD, Pourghasemi HR et al (2013) Landslide susceptibility mapping using certainty factor, index of entropy and logistic regression models in GIS and their comparison at Mugling–Narayanghat road section in Nepal Himalaya. Nat Hazards 65(1):135–165

Du GL, Zhang YS, Lv WM et al (2016) Landslide susceptibility assessment based on weighted information value model in Southeast Tibet. J Catastrophol 31(2):226–234 (In Chinese)

Du GL, Zhang YS, Iqbal J et al (2017a) Landslide susceptibility mapping using an integrated model of information value method and logistic regression in the Bailongjiang watershed, Gansu Province, China. J Mt Sci 14(2):249–268

Du GL, Zhang YS, Yang ZH et al (2017b) Estimation of seismic landslide Hazard in the eastern Himalayan Syntaxis region of Tibetan plateau. Acta Geol Sin (English Edition) 91(2):658–668

Ercanoglu M, Kasmer O, Temiz N (2008) Adaptation and comparison of expert opinion to analytical hierarchy process for landslide susceptibility mapping. Bull Eng Geol Environ 67(4):565–578

Fan LF, Hu RL, Zeng FC et al (2012) Application of weighted information value model to landslide susceptibility assessment - a case study of Enshi city, Hubei province. J Eng Geol 20(4):508–513 (In Chinese)

Feizizadeh B, Roodposhti M S, Jankowski P, et al (2014) A GIS-based extended fuzzy multi-criteria evaluation for landslide susceptibility mapping. Comput Geosci 73:208–221

Fenta AA, Kifle A, Gebreyohannes T, Hailu G (2015) Spatial analysis of groundwater potential using remote sensing and GIS-based multicriteria evaluation in Raya Valley, northern Ethiopia. Hydrogeol J 23(1):195–206

Gallo F, Lavé J (2014) Evolution of a large landslide in the high Himalaya of Central Nepal during the last half-century. Geomorphology 223:20–32

Ghosh S, Carranza EJM, Van Westen CJ et al (2011) Selecting and weighting spatial predictors for empirical modeling of landslide susceptibility in the Darjeeling Himalayas (India). Geomorphology 131(1):35–56

Godt JW, Baum RL, Savage WZ et al (2008) Transient deterministic shallow landslide modeling: requirements for susceptibility and hazard assessments in a GIS framework. Eng Geol 102(3–4):214–226

Guo CB, Montgomery DR, Zhang YS et al (2015) Quantitative assessment of landslide susceptibility along the Xianshuihe fault zone, Tibetan plateau, China. Geomorphology 248:93–110

Hasekiogullari GD, Ercanoglu M (2012) A new approach to use AHP in landslide susceptibility mapping: a case study at Yenice (Karabuk, NW Turkey). Nat Hazards 63(2):1157–1179

Hong H, Liu J, Bui DT et al (2018) Landslide susceptibility mapping using J48 decision tree with AdaBoost, bagging and rotation Forest ensembles in the Guangchang area (China). Catena 163:399–413

Kayastha P, Dhital MR, De SF (2013) Application of the analytical hierarchy process (AHP) for landslide susceptibility mapping: a case study from the Tinau watershed, West Nepal. Comput Geosci 52:398–408

Lan HX, Zhou CH, Wang LJ et al (2004) Landslide hazard spatial analysis and prediction using GIS in the Xiaojiang watershed, Yunnan, China. Eng Geol 76(1):109–128

Lee S, Pradhan B (2006) Probabilistic landslide hazards and risk mapping on Penang Island, Malaysia. J Earth Syst Sci 115(6):661–672

Lee S, Talib JA (2005) Probabilistic landslide susceptibility and factor effect analysis. Environ Geol 47(7):982–990

Lin ML, Tung CC (2004) A GIS-based potential analysis of the landslides induced by the chi-chi earthquake. Eng Geol 71(1):63–77

Liu GR, Yan EC, Lian C (2002) Discussion on classification of landslides. J Eng Geol 10(4):339–342 (in Chinese)

Meinhardt M, Fink M, Tünschel H (2015) Landslide susceptibility analysis in Central Vietnam based on an incomplete landslide inventory: comparison of a new method to calculate weighting factors by means of bivariate statistics. Geomorphology 234:80–97

Meng H, Zhang YQ, Yang N (2004) Analysis of the spatial distribution of geohazards along the middle segment of the eastern margin of the Qinghai-Tibet plateau. Geol China 31(2):218–224 (In Chinese)

Mezughi TH, Akhir JM, Rafek AGM et al (2011) Landslide susceptibility assessment using frequency ratio model applied to an area along the EW highway (Gerik-Jeli). Am J Environ Sci 7(1):43–50

Mondal S, Maiti R (2013) Integrating the analytical hierarchy process (AHP) and the frequency ratio (FR) model in landslide susceptibility mapping of shiv-khola watershed, Darjeeling Himalaya. Int J Disas Risk Sci 4(4):200–212

Park NW (2010) Application of Dempster-Shafer theory of evidence to GIS-based landslide susceptibility analysis. Environ Earth Sci 62(2):367–376

Park HJ, Lee JH, Woo I (2013) Assessment of rainfall-induced shallow landslide susceptibility using a GIS-based probabilistic approach. Eng Geol 161:1–15

Pourghasemi HR, Moradi HR, Aghda SMF (2013) Landslide susceptibility mapping by binary logistic regression, analytical hierarchy process, and statistical index models and assessment of their performances. Nat Hazards 69(1):749–779

Pradhan B, Lee S (2010) Landslide susceptibility assessment and factor effect analysis: backpropagation artificial neural networks and their comparison with frequency ratio and bivariate logistic regression modelling. Environ Model Softw 25(6):747–759

Regmi AD, Yoshida K, Pourghasemi HR et al (2014) Landslide susceptibility mapping along Bhalubang-Shiwapur area of mid-Western Nepal using frequency ratio and conditional probability models. J Mt Sci 11(5):1266–1285

Sarkar S, Kanungo DP, Patra AK et al (2008) GIS based spatial data analysis for landslide susceptibility mapping. J Mt Sci 5(1):52–62

Shang YJ, Park HD, Yang ZF et al (2005) Distribution of landslides adjacent to the northern side of the Yarlu Tsangpo grand canyon in Tibet, China. Environ Geol 48(6):721–741

Sharma M, Kumar R (2008) GIS-based landslide hazard zonation: a case study from the Parwanoo area, lesser and outer Himalaya, H.P., India. Bull Eng Geol Environ 67(1):129–137

Suh J, Choi Y, Roh TD et al (2011) National-scale assessment of landslide susceptibility to rank the vulnerability to failure of rock-cut slopes along expressways in Korea. Environ Earth Sci 63(3):619–632

Tahmassebipoor N, Rahmati O, Noormohamadi F et al (2016) Spatial analysis of groundwater potential using weights-of-evidence and evidential belief function models and remote sensing. Arab J Geosci 9(1):1–18

Tsangaratos P, Ilia I (2016) Comparison of a logistic regression and Naïve Bayes classifier in landslide susceptibility assessments: the influence of models complexity and training dataset size. Catena 145:164–179

Umar Z, Pradhan B, Ahmad A et al (2014) Earthquake induced landslide susceptibility mapping using an integrated ensemble frequency ratio and logistic regression models in west Sumatera Province, Indonesia. Catena 118:124–135

Wang F, Xu P, Wang C et al (2017) Application of a GIS-based slope unit method for landslide susceptibility mapping along the Longzi River, southeastern Tibetan plateau, China. ISPRS Int J Geo-Inform 6(6):172

Yang ZH, Lan HX, Gao X et al (2015) Urgent landslide susceptibility assessment in the 2013 Lushan earthquake-impacted area, Sichuan Province, China. Nat Hazards 75(3):2467–2487

Yao X, Tham LG, Dai FC (2008) Landslide susceptibility mapping based on support vector machine: a case study on natural slopes of Hong Kong, China. Geomorphology 101(4):572–582

Yilmaz I (2009) A case study from Koyulhisar (Sivas-Turkey) for landslide susceptibility mapping by artificial neural networks. Bull Eng Geol Environ 68(3):297–306

Yilmaz I (2010) Comparison of landslide susceptibility mapping methodologies for Koyulhisar, Turkey: conditional probability, logistic regression, artificial neural networks, and support vector machine. Environ Earth Sci 61(4):821–836

Yilmaz I, Keskin I (2009) GIS based statistical and physical approaches to landslide susceptibility mapping (Sebinkarahisar, Turkey). Bull Eng Geol Environ 68(4):459–471

Yin KL, Yan TZ (1988) Statistical prediction model for slope instability of metamorphosed rocks[C]//proceedings of the 5th international symposium on landslides, Lausanne. Switzerland 2:1269–1272

Yin KL, Yan TZ (1996) Landslide prediction and relevant models. Chin J Rock Mech Eng 15(1):1–8 (In Chinese)

Youssef AM, Pradhan B, Jebur MN et al (2015) Landslide susceptibility mapping using ensemble bivariate and multivariate statistical models in Fayfa area, Saudi Arabia. Environ Earth Sci 73(7):3745–3761

Zhou SH, Wang W, Chen GQ et al (2016) A combined weight of evidence and logistic regression method for susceptibility mapping of earthquake-induced landslides: a case study of the April 20, 2013 Lushan earthquake, China. Acta Geol Sin (English Edition) 90(2):511–524